



0601

SWELLING AND ANOMALOUS DIFFUSION MECHANISMS OF CO₂ IN COAL

Saikat Mazumder, Johannes Bruining and Karl Heinz Wolf
Department of Geotechnology, Delft University of Technology,
The Netherlands

ABSTRACT

We propose a theory to explain the diffusion process of CO₂ in coal and its relation to matrix swelling. The swelling of coal matrix by the sorption of CO₂ is characterized by an anomalous diffusion process. We suggest the application of theories of sorption behaviour of polymers for coals. The mechanism of CO₂ diffusion in coal can be determined by a variety of experimental techniques. Considering the fact that swelling is proportional to the amount of material that has diffused into the matrix, the dimensionless mass uptake curve can be plotted against time according to the equation $M_t/M_e \approx kt^n$. If the diffusion exponent n is 0.5 (for planar systems) the diffusion is Fickian. Non-Fickian / anomalous behavior is observed for $0.5 < n < 1.0$, with a limit of Case II transport for $n = 1.0$. Anomalous and Case II diffusion are indicative of the coupling of diffusional and relaxational mechanisms. Relaxation is related to the transition of coal from glassy to a rubbery state. Major relaxational mechanisms are indicative of swelling related stresses in coal. The diffusion exponent for a Warndt Luisenthal coal sample has been experimentally determined having values inbetween 0.7 and 0.8. A mathematical model is presented, which can be used to describe the anomalous transport of CO₂ in thin coal slabs. Parameters specific to a CO₂ - coal system have been determined and simulation results will be presented. The sharp diffusion front which is a characteristic of Case II diffusion is observed and results from a discontinuity in the diffusivity - concentration relationship. This model will be useful in defining anomalous transport behavior of CO₂ in the macromolecular network structure of coal.

INTRODUCTION

Maturation of coalbed methane (CBM) production operations in some basins and the emergence of injection schemes for enhanced coalbed methane (ECBM), and carbon sequestration of greenhouse gases has led to renewed focus on the behavior of coalbed reservoir properties under these conditions. Coal swelling accompanying CO₂ sorption would decrease the permeability of the coal as the volume increase is compensated within the fracture porosity.

The "swelling" of coal by a penetrant can be referred to as, an increase in the volume occupied by the coal as a result of the viscoelastic relaxation of its highly crosslinked macromolecular structure. Although the macro molecular network structure doesnot dissolve, the penetrant is almost universally termed as "solvent". Thus a coal - coal hydrogen bond or any other weaker bond will be replaced by a coal-solvent bond only if the new coal-solvent bond is thermodynamically favoured. If intramolecular bonding in the coal contributes significantly to its structural integrity, then strong coal-solvent bonding should disrupt such a structure, which results into coal swelling.

A CO₂ molecule placed between the polymer chains of coal disrupts partly the original structure if the sorption takes place in locations where the available volume between the chains is smaller than the actual volume of the CO₂ molecule. This disruption requires energy to overcome attractive forces between the chains, which can be described in the form of Lennard-Jones potentials and coulombic electrostatic potentials. Furthermore, the energy

which is required to change the conformation of the polymer chains: rotational alterations of sp³-bonds and out-of-plane bending of sp²-bonds will be responsible for the change of the chain conformation.

The similarities in structure between coal and glassy polymers have led us to the perception that CO₂ penetration has many analogous features that are observed for organic sorbents penetrating into glassy polymers. In other words we propose the application of theories of sorption behaviour of polymers to coals. For the interpretation of the experiments we assume that a matrix slab of more or less constant thickness exists between cleats.

During penetrant transport at low or moderate temperatures, into the macromolecular network of coal, the network density decreases which results into an increase of the large molecular chain motions [1]. This increase of the penetrant concentration of the network can be viewed as an effective decrease of the glass transition temperature [2]. Structural changes induced during this process include swelling, microcavity formation and primary phase transition requiring rearrangements of each chain segments. Such changes are dominated by relaxational phenomenon.

The diffusion of gas into glassy polymers varies between two extremes. If the diffusion is controlled by the concentration gradient between the centre and the outside of the coal matrix, the diffusion mechanism is Fickian. If the transport is controlled by a stress gradient induced by the penetration of molecules the diffusion mechanism is anomalous. For polymers the following observations are made.

The diffusion in glassy polymers often does not fit the Fickian diffusion model. Alfrey, Gurnee and Lloyd [3] have presented a second limiting case for sorption, where the rate of transport is entirely controlled by molecular relaxation. This type of transport mechanism is designated as Case II transport. The characteristics of Case II diffusion in coal are as follows:

(a) The penetrant is observed to advance through the macromolecular glassy substance with a sharp upstream boundary to a rubber zone. Downstream the penetrant concentration is zero. Upstream the rubber zone the penetrant is at equilibrium concentration. The rubber part is substantially swollen with respect to the glassy part.

(b) After some initializing effects a semi-steady state occurs, where a given concentration profile travels through the slab

(c) The boundary between the swollen matrix and the glassy material advances at a constant velocity.

(d) The initial weight gain of the sample has a linear propagation with time.

(e) The swollen matrix behind the advancing front is at a uniform state of swelling.

(f) Many authors state that the Fickian flux of solvent must be supplemented by a flux due to stress gradient which exists across the moving boundary.

(g) Some process of molecular relaxation is possible for control of the front velocity.

(h) Peterlin [4] suggests that the sharp diffusion front, characteristic of the Case II process, is preceded by a region of penetrant at low concentration which forms a precursor to the front and results from Fickian diffusion into the glassy material ahead of the front. He recognizes that the velocity of the front is controlled by some independent material property, and suggests time dependent rupture and disentanglement of molecular chains as a possible process.

(i) Thomas and Windle [5] proposed that the rate controlling step at the penetrant front is the time dependent mechanical deformation of the glassy polymer in response to the thermodynamic swelling stress.

Most transport processes in coal can be represented by a coupling of the Fickian and Case II transport mechanisms. A simple expression of this observation can be written by adding the diffusion controlled to relaxation controlled uptakes:

$$\frac{M_t}{M_e} = k_1 \sqrt{t} + k_2 t \approx kt^n \quad (1)$$

where M_t is the mass uptake at time t and M_e is the equilibrium mass uptake, k is a constant incorporating characteristics of the macromolecular network system and the penetrant, and n is the diffusional exponent, which is indicative of the transport mechanism. Eq. (1) is valid for the first 60% of the normalized penetrant uptake. Fickian diffusion and Case II transport for a thin slab are defined by n equal to 0.5 and n equal to 1 respectively. Anomalous transport behavior is intermediate between Fickian and Case II, and has a value of n between 0.5 and 1. The geometry of the sample plays an important role in determining the value of the diffusion exponent n . An analysis of the geometry of the particle with the diffusion exponent has been done by Ritger et al. [1]. The results from this analysis show that Fickian diffusion and Case II transport in a cylindrical sample (inside to outside) are defined by $n = 0.451 \pm 0.004$ and $n = 0.89 \pm 0.02$ respectively. Similar analysis was performed on the first 60% of

the sorption process for Fickian diffusion and Case II transport in a spherical sample. The results of this analysis show that Fickian diffusion and Case II transport are defined by $n = 0.432 \pm 0.007$ and 0.85 ± 0.02 respectively.

Vrentas et al. [6, 7] introduced the Deborah number (D_e) as a means of characterizing penetrant uptake. In terms of D_e , the nature of the sorption process can be distinguished by the ratio of two characteristic times, namely (i) λ , for the macromolecular penetrant system; and (ii) a characteristic diffusion time, θ . The Deborah number is written as,

$$D_e = \frac{\lambda}{\theta} \quad (2)$$

The dependence of Deborah number and diffusional exponent on sample geometry is shown in Table. 1. For $D_e \gg 1$, i.e. relaxation time much larger than diffusion time, there is effectively no time variation of the macromolecular structure during the diffusion process. Such a sorption process can be described by Fickian diffusion. For $D_e \ll 1$, i.e. relaxation time much smaller than diffusion time, conformational changes in the macromolecular structure occur instantaneously with respect to the time scale of diffusion. This type of sorption process is also described by Fickian diffusion. Hence, in relation to the diffusional exponent n , systems exhibiting $D_e \gg 1$ or $D_e \ll 1$ can be characterized by n equal to 0.5 (for slab geometry). When $D_e = 0(1)$, i.e. the relaxation and diffusion times are of the same order of magnitude, case II diffusion becomes relevant. As the penetrant diffuses into the macromolecular network, rearrangement of the chains does not occur immediately. Thus, the instantaneous macromolecular configuration may differ from the equilibrium network structure at the same penetrant concentration. This situation represents anomalous transport behavior, which is defined by values of n between 0.5 and 1. When $D_e = 1$, uptake is controlled by macromolecular chain relaxation only. This value of D_e represents Case II transport where the diffusional exponent is equal to 1. It has been reported that the transport mechanism observed for a coal / penetrant system depends on the sample dimensions. This phenomenological observation can be interpreted in terms of the diffusional Deborah number in the following way. A characteristic diffusion time for one dimensional diffusion in thin films is defined as,

$$\theta \cong \frac{\delta^2}{D} \quad (3)$$

where the characteristic diffusion length, δ , is the film half thickness, $l/2$, and D is the gas diffusion coefficient in the macromolecular structure. Thus, the diffusional Deborah number can be written as,

$$D_e \cong \frac{\lambda D}{l^2} \quad (4)$$

These presumptions, that anomalous diffusion is the prevailing transport mechanism for CO_2 in coal, are verified in our experiments.

DYNAMIC VOLUMETRIC SWELLING EXPERIMENTS

The diffusion process is closely interlinked to the dynamic volumetric swelling (DVS) of coal. The increase in volume of a coal sample is a function of time. Only the adsorbent that has diffused into the "bulk" structure induces coal swelling. The increase in volume is proportional to the amount of material that has diffused into the "bulk". This process disregards all occluded sorbents. At any time t , the amount of adsorbent that has diffused into the "bulk" is proportional to the volumetric swelling. S_t is the amount of volumetric swelling at time t , and S_e is the equilibrium swelling. The variation of mass uptake with time has the same apparent functional variation for Fickian and relaxation diffusion. To distinguish graphically between the extreme modes of diffusion (bounds) it is conventional to plot the dimensionless mass uptake (S_t/S_e) as a function of the square root of the dimensionless time (t/t_e) (Fig. 1). The Fickian curve increases monotonically, whereas the relaxation controlled mode has an inflection at low $(t/t_e)^{1/2}$ (Fig. 1).

Equipment design and sample preparation

The set-up was designed to measure volumetric strain due to changes in sorbed gas concentration while keeping the net stress on the coal sample constant. The uniqueness of these experiments, using large cores, makes the design of the setup complex. A high-pressure core flooding setup was constructed. The pressure cell can reach a maximum confining pressure of 500 bars. The confining pressure as can be otherwise stated as the outside mechanical stress was exerted by means of hydraulic oil. During the course of the experiment this confining pressure was controlled manually so as to set the required effective stress (P_{eff}). For each pressure step the expected pore pressure was calculated and then the confining pressure was added manually by means of a pressure actuated valve to keep the effective stress (P_{eff}) constant throughout the course of the experiment. The confining pressure was applied on the coal core, inside a rubber sleeve. To prevent the gas from diffusing through the rubber sleeve, a lead foil was wrapped around the coal core. To simulate downhole conditions the temperature in the pressure cell was maintained at 45°C. The sample diameter is 72 mm. The length of the core varied from sample to sample. For the DVS experiment a low rank coal core of 154 mm in length was used. The schematic of the setup is shown in Fig. 2. A reference vessel, outside the reactor was used to feed the gas. The gas was charged to this reference vessel by an ISCO pump. Then the gas was boosted into the reference cell, to get the required pressures. Time was needed to stabilize the temperature in the reference cell.

Strain gauges were attached on the sample surface to measure the sorption induced volumetric strain in the coal. The strain measurements were stored, through an amplifier and a data acquisition system, into a computer. Dynamic strain measurement is done with the four strain gauges connected to an amplifier and data acquisition system. The sample used for these experiments was from the Warndt Luisenthal coalfield in Germany. The detail of the sample is shown in Table 2.

First, a part of the coal core surface, smoothed free of cleats, was selected. If needed, the representative surface was polished. So that the strain gauges did not come off the surface due to the shear force of the rubber sleeve, grooves of about 2 mm deep were made. The groove surfaces were also polished. The bonding area was cleaned with industrial tissue paper or cloth soaked in a small quantity of chemical solvent such as acetone. It was cleaned until a new tissue or cloth comes away completely free of coal particles. If the surface is left uneven, the strain gauges will not adhere properly to the surface. Then the adhesive to be used for fixing the strain gauges on the coal surface was prepared. The adhesive was applied evenly on both the surfaces, i.e. on the strain gauge surface as well as the coal surface. A polyethylene sheet was placed onto it and pressed down on the gauge for about 10 minutes. Connectors were positioned at a distance of 3 to 5 mm from the gauge. The junction area was soldered for both the gauge leads and the connecting terminals. To connect the extension, the lead wires were soldered to the connecting terminals. Two strain gauges were axially oriented and the two other radially on the core surface. Copper wires of sufficient length were soldered to the terminals of each of these strain gauges. A groove was made along the length of the core & the wires were guided through this groove. All the grooves were then filled with a mixture of coal puff and the adhesive. This further prevented the strain gauges from being sheared off the surface during the experiment.

The strain gauges were of the rosette type (TML-PC-10) gauges, with a gauge factor of 2.07. The strain gauges had an accuracy of +/- 2 %. The gauge factor can be defined as follows:

$$k = \frac{\Delta R / R}{\varepsilon} \quad (5)$$

$\Delta R/R$ is indicated by specifying the Poisson's ration of the test specimen. The gauges were connected to a (1/4) Wheatstone bridge, whose aplifier output is given by:

$$\varepsilon = \frac{4A_{op}}{k\mu_B A} \quad (6)$$

With this arrangement, the axial and radial strain in the coal sample due to the dynamic swelling induced by the sorption of CO₂ was measured. The directional placements of the strain gauges were done, so as to measure

the two horizontal strains (strain parallel to the bedding plane). Since the natural fracture system in coal (cleats) is disposed perpendicular to the bedding plane, it's the horizontal strain which is involved in permeability change taking place due to the swelling of the coal matrix. Assuming isotropic stress conditions, the volumetric strain for the coal core was calculated as follows:

$$\varepsilon_v = (1 + \varepsilon_a)(1 + \varepsilon_r)^2 - 1 \quad (7)$$

where ε_v , ε_a and ε_r are volumetric, axial and radial strains respectively.

Results and discussion

Dynamic volumetric swelling (DVS) experiments were performed on a Warndt Luisenthal coal core (0.71% R_{max}) with CO_2 at 45°C. The tests start with a complex procedure of mounting the coal core sample in a rubber sleeve and building it in the high-pressure cell; leak free. The sample cell was connected to a vacuum pump, for at least a week, to eliminate any form of residual gas or moisture. Prior to the start of the experiment, strain gauges were calibrated for temperature variations. During an experiment the CO_2 is fed in the pressure cell to a certain pressure and the pressure is allowed to equilibrate over time. A DVS measurement on the first Warndt Luisenthal experiment is shown in Fig. 3. The plots correspond to the experimental data from the first pressure step. The pressure decline curve corresponds to the uptake of CO_2 and is assumed to be proportional to the dynamic volumetric swelling. A repeat Warndt Luisenthal experiment is performed and the the DVS measurement is shown in Fig. 6. In Figs. 4 and 7 the equilibrium swelling ratio is plotted against the square root of the dimensionless time. Assuming that mass uptake is proportional to the amount of swelling observed, and using Eq. (1), the transport phenomenon of CO_2 in coal can be determined. Graphs of $\ln[(S_e - S_t)/S_e]$ against time, for the first and the repeat Warndt Luisenthal experiments are shown in Figs. 5 and 8. To determine the mechanism of initial diffusion of CO_2 into the coal, the data from the initial CO_2 swelling region were fitted to Eq. (1), where k is a constant and n is the diffusion exponent. Values of $0.5 < n < 1$ the diffusion is anomalous. For the first and the repeat Warndt Luisenthal experiment, diffusion exponents of 0.78 and 0.72 were calculated respectively. These results are a clear indication towards the fact that CO_2 diffusion in coal is anomalous in nature. Thus the ability of CO_2 to disrupt weak bonds in coal and thereby cause swelling of the macromolecular structure is depicted. However this transport process is highly dependent on the geometry of the sample. It has to be noted that sorption curves generated from diffusion experiments on grounded coal samples are not representative of the true geometry under insitu conditions. Swelling of coal by CO_2 is the outcome of a relaxation driven anomalous diffusion process.

To understand the physics behind such a complex relaxation driven diffusion process, a simple 1D model have been presented. No efforts have been made to validate the experimental results with the present model.

A CASE II DIFFUSION MODEL IN COAL

Coal has a large capacity to sorb, and transform in the process from a stiff glassy coal to a rubbery solid. Unlike the Fickian diffusion, the penetration of a sorbent molecule into coal is accompanied by swelling. The Thomas and Windle model stimulated experimental research of Case II sorption, particularly by Kramer et al. [8, 9] on a number of polymer/sorbent systems using the Rutherford backscattering technique. Hui et al. [10, 11] dealt with both the initial transient penetration of the sorbent and the final steady state motion of the sorption front - all within the framework of the Thomas and Windle model. The experiments and these more detailed models showed that while the Thomas and Windle model has a successful qualitative framework of most of the important mechanistic factors, it is unable to provide a quantitatively accurate statement of the kinetics of the sorbent penetration. The later requires a more highly non-linear material deformation resistance. There has been a number of other model developments of Case II sorption such as, e.g. of Govindjee et al. [12] that emphasizes the representation of the thermodynamic driving forces arising from activity gradients and a glass to rubber transition. As a distinguishing feature of Case II sorption is the associated material misfit produced by the sorbent, the development of internal stresses must be an important component of the process. Alternatively, there must be present effects of applied external stresses or pressures, which accelerate or retard the diffusion process. Thomas and Windle [5] have rightly noted that the presence of an imposed negative pressure will enhance the equilibrium of the sorbent in the glassy coal at a given temperature significantly. Durning [13] extended the Thomas and Windle model using linear irreversible thermodynamics. They replaced the viscous model with the Maxwell viscoelastic model, so that a relaxation time can be defined. The relation between osmotic pressure and

the stresses on the coal was analyzed using the force balance. Argon et al. [14] presented a mechanistic model, which considers the conditions that govern the self-similar propagation of fully developed Case II sorption fronts, combined with their Fickian precursors. The principal point of departure from all other models is the specific considerations of the effects of the sorbent induced material misfit and the non-linear viscoelastic response of the constrained coal matrix to the misfit induced effective stresses. This stress has been termed as the swelling stress (P_{xx}), and is defined as the pressure of an element of coal matrix saturated with the adsorbent (CO₂/CH₄/N₂) avoiding at the same time deformation. The very definition makes it clear that the measurement, or measurement methodology of swelling stress, is not a matter to be easily accomplished. From the viewpoint of thermodynamics, swelling stress represents a kind of energy. In the case of free swelling (unconstrained laboratory conditions) it turns out to be a volume change (dV). Swelling stress only occurs in the case of constrained swelling. The concept of swelling stress is shown in Fig. 9. Considering a deformed domain, a process of back compaction can be visualized to understand the swelling stress (P_{xx}).

Model equations

The Thomas and Windle model is able to predict successfully, the essential aspects of Case II diffusion. The model proposes that the diffusive process is strongly coupled to the mechanical response of coal. This happens in a sense that the rate at which the penetrant is absorbed must be compatible with the swelling rate, controlled by the creep deformation of the surrounding coal. It is a diffusion which is stress driven. The creep deformation depends on both the osmotic pressure, which drives the swelling, and the viscosity of the material. The viscosity and diffusivity of the coal are extremely sensitive to the concentration of the penetrant. The penetrant produces very large decreases in viscosity and increases in diffusivity within a very narrow range of concentration (Fig. 10). These changes are due to plasticization caused by sorption of the penetrant, which produces a decrease in coal segmental relaxation times from very large, glassy behavior, to very short, rubbery behavior. It is this strong dependence of viscosity and diffusivity on penetrant concentration that produces the sharp front which is a characteristic of Case II or anomalous diffusion [5].

The salient features of the Thomas and Windle (TW) model are well summarized by Hui et al. [10, 11]. Since Case II diffusion is introduced for coal for the first time, a short explanation is needed. According to the TW model, the concentration (volume fraction) Φ of the penetrant only depends on one spatial dimension x , i.e. $\Phi = \Phi(x, t)$, where t denotes time. The increase in the concentration occurs by the penetrant molecules occupying "interstitial" sites between polymer chains in the coal. To a good approximation the glassy coal is a random close-packed arrangement of chain segments with little "free volume". There are only a limited number of such sites that may be occupied without the concurrent motion of the crosslinkings. If the equilibrium volume fraction of penetrant is larger than the volume fraction of the existing interstitial sites, there is a kinetic problem associated with the sorption. As compared to the glassy state of coal, in the rubbery state the crosslink polymeric chains can move separately and rapidly by process involving rotation of main chain bonds so that the equilibrium is obtained almost instantaneously. Thus, the initial penetrant volume Φ will be less than the equilibrium volume fraction Φ_0 . Φ approaches this value only as permitted by the motion of the polymeric chains in coal.

Thomas and Windle [5] treat the swelling rate, or the rate of change of volume fraction of penetrant, as the rate of linear viscous creep deformation driven by the osmotic pressure, P_{xx} . The amount of penetrant is expressed in terms of the volume fraction Φ , which is related to the concentration by $\Phi = c/\Omega$, where Ω is the partial molecular volume.

We summarize their derivation here with the help of the article by Hui et al. [10, 11] and the book on "Extended Irreversible Thermodynamics" by Jou et al. [16]. Classical non-equilibrium thermodynamics (CIT) shows no coupling of concentration gradients and viscous stress gradients as they are of different tensorial character. Extended non-equilibrium thermodynamics show that the molar (diffusive) flux J is not only driven by the volume fraction gradient $\partial\Phi/\partial x$, but also by the stress gradient $\partial P_{xx}/\partial x$ [17] i.e.

$$J = -D \frac{\partial}{\partial x} \left(\phi + \frac{\Omega \phi}{k_B T} P_{xx} \right) \quad (8)$$

The coefficients are determined by comparison to CIT. P_{xx} is interpreted as the stress that balances the osmotic pressure Π i.e. $P_{xx} = -\Pi$.

Vice versa also the stress is related to molar flux gradient as

$$P_{xx} = -\eta_l \frac{\partial J}{\partial x} = \eta_l \frac{\partial \phi}{\partial t} \quad (9)$$

Where η_l is the elongational viscosity and Ω is the partial molar volume. The second equation follows from the mass balance equation

$$\frac{\partial \phi}{\partial t} + \frac{\partial J}{\partial x} = 0 \quad (10)$$

The diffusion coefficient depends on the concentration. Below a critical volume fraction Φ_c a diffusion coefficient D_g characteristic of a glassy state is used, and above Φ_c the diffusion coefficient D_r , characteristic of the rubber (swollen) state is used. It can be expected that $D_r / D_g \gg 1$. In the model an abrupt change of the diffusion coefficients at Φ_c is used, but D_r and D_g are considered constant for $\Phi > \Phi_c$ and $\Phi < \Phi_c$ respectively.

Therefore we find after substituting into Eq. (8),

$$J = -D \frac{\partial}{\partial x} \left(\phi + \frac{\eta_l \Omega \phi}{k_B T} \frac{\partial \phi}{\partial t} \right) \quad (11)$$

and after substituting into the mass balance equation, Eq. (10) we arrive at

$$\frac{\partial \phi}{\partial t} = \frac{\partial}{\partial x} D \frac{\partial}{\partial x} \left(\phi + \frac{\eta_l \Omega \phi}{k_B T} \frac{\partial \phi}{\partial t} \right) \quad (12)$$

The elongational viscosity η_l is supposed to depend on the volume fraction of the penetrant as

$$\eta_l = \eta_0 \exp(-m\phi) \quad (13)$$

Where m is a material constant and η_0 is the volumetric viscosity of the unswollen coal sample. The final equilibrium concentration is reached when the coal has swollen to make the stress P_{xx} equal to zero. In this case the volume fraction of CO_2 in the coal is in equilibrium with the CO_2 in the fluid phase outside the coal. Also the CO_2 in the stressed coal is in equilibrium with the CO_2 in the fluid phase. The change in chemical potential $d\mu = -\Omega dP_{xx} + k_B T d \ln \Phi$. Here we use that the stress is equal to minus the osmotic pressure. Equating the chemical potential in the unstressed and stressed state leads to:

$$-\Omega P_{xx} + k_B T \ln \phi = -\Omega P_{xx}^0 + k_B T \ln \phi_0 \quad (14)$$

Substitution of Eq. (9) and Eq. (13) into Eq. (14) leads to

$$\ln \phi / \phi_0 = \frac{\eta_0 \Omega}{k_B T} \exp(-m\phi) \frac{d\phi}{dt}. \quad (15)$$

The solution to this equation is

$$t = \phi_0 \frac{\eta_0 \Omega}{k_B T} \int_0^{\phi/\phi_0} \frac{\exp(-m\phi_0 y)}{\ln y} dy \quad (16)$$

Where we use the boundar condition that $\Phi = 0$ at $t = 0$.

Steady-state solution

Hui et al. [10, 11] showed that Eq. (12) can have a traveling wave like solution if the diffusion coefficient in the glass state (initial coal) approaches zero. This means that the velocity of the volume fraction Φ_c at which the transition between the glass state and the rubbery state occurs, is initially proportional to time. To solve the problem of a steadily moving front, the following assumptions are made regarding the diffusivity. Let D_g and D_r denote the diffusivity of the coal in the glassy and the rubbery states respectively, brought about by the plasticization of the coal with the imbibition of CO₂. We assume that there exists a critical concentration Φ_c , such that, for $\Phi < \Phi_c$, $D(\Phi) \approx D_g$ and for $\Phi > \Phi_c$, $D(\Phi) \approx D_r$ and that $D_r \gg D_g$. We also assume that the transition from D_g to D_r takes place within a narrow range of Φ about Φ_c , and $D(\Phi)$ is a monotonically increasing function of Φ . We use a conventional finite volume representation of Eq. (12). We use the initial conditions that $\Phi(x)$ and $\partial\Phi/\partial t(x)$ are zero. The boundary condition at the end of the slab ($x=L$) is $(\partial\Phi/\partial x)(L)=0$ and at $x=0$, we obtain the volume fraction $\Phi(x=0)$ from Eq. (16). The parameters used for the simulation are summarized in Table 3. The result from the simulation is shown in Fig. 11. The choices for the parameters were made so that they are both typical and reasonable for coal. Considering the difficulty in the exact assesment of parameters, the fact that calculated kinetics is those typical of Case II diffusion, is encouraging. Fig. 11 shows the effect on the calculated profiles of the changing m . It is a material constant and is a factor that controls the 'steepness' of the exponential dependence of viscosity. When m decreases, the profiles become more closely spaced. It indicates that the sorption rate is dropping off. This behavior is confirmed by the total sorption plots in Fig. 11. The step like profiles can result from a discontinuity in the diffusivity - concentration relationship. A parameter sensitivity analysis is presently being carried out.

CONCLUSIONS

- A comprehensive details about the highly crosslinked macromolecular nature of coal has been presented.
- Experiments have been conducted to determine the diffusion exponent (n) in coal, with respect to CO₂ sorption. The first pressure steps and the corresponding mass uptake curves have been used. Diffusion expont between 0.7 and 0.8 have been calculated and it distictively suggest an anomalous diffusion process. More experiments to understand the diffusion process under stressed condition needs to be carried out.
- A theory is introduced that accounts for the phenomenon of anomalous diffusion which is observed when bituminous coal swells in CO₂. The theory explains the process in terms of the contrast in the diffusion coefficients (D_r and D_g) and the viscosity of the unswollen coal (η_0).
- A solution to the TW model pertaining to Case II diffusion has also been presented. The derivation of the model with inputs from extended non-equilibrium thermodynamics have been used in conjunction with the work of Hui et al. [10, 11].
- Parameter estimation for the model corresponding to the diffusion of CO₂ in coal has been done.

- Sharp concentration fronts in line with the theory of Case II diffusion has been observed in the simulation results.

NOMENCLATURE

M_t = dimensionless mass uptake [-],
 M_e = equilibrium mass uptake [-],
 k = constant incorporating characteristics of the macromolecular network system and the penetrant [-],
 n = diffusional exponent [-],
 D_e = Deborah number [-],
 λ = characteristic time for the macromolecular penetrant system [s],
 θ = characteristic diffusion time [s],
 δ = characteristic diffusion length [m],
 l = film thickness [m],
 D = gas diffusion coefficient [m^2/s],
 ε = strain [-],
 S_t = amount of volumetric swelling at time t [-],
 S_e = equilibrium swelling at time t_e [-],
 Φ = volume fraction of the penetrant [-],
 Φ_0 = equilibrium volume fraction [-],
 P_{xx} = viscous stress [kg/m^2],
 η_l = elongational viscosity of coal [Ns/m^2],
 η_0 = volumetric viscosity of the unswollen coal sample [Ns/m^2],
 Ω = partial molar volume of CO_2 [$m^3/molecule$],
 m = material constant [-],
 D_g = diffusion coefficient characteristic of a glassy coal [m^2/s],
 D_r = diffusion coefficient characteristic of a swollen (rubbery) coal [m^2/s],
 Φ_c = critical volume fraction [-],
 k_B = Boltzman constant [$1.37983 \times 10^{-23} J/molecule/K$],
 T = temperature [K],
 μ = chemical potential,
 L = slab length [m]

ACKNOWLEDGEMENTS

This work was funded by the CO_2 sequestration project "RECOPOL", the Dutch "CATO" and the "NWO-NOVEM" programme. At the very onset, we would like to thank Prof. Harpalani from the University of Southern Illinois, Carbondale, Prof. Dan Marchesin from IMPA, Rio de Janeiro, Brazil and Sijmon van der Wal from Diffusion-polymers.com for their valuable input. They have been instrumental in solving our doubts, which have been basic at times. My special thanks to Henk van Asten and Leo Vogt for their technical support. The experimental work would not have been possible without their help.

REFERENCES CITED

1. Ritger, P. L. and Peppas, N. A., 1987: "Transport of penetrants in the macromolecular structure of coals"; Fuel 66, 815-826.
2. Hsieh, S. T. and Duda, L. J., 1987: "Probing coal structure with organic vapour sorption"; Fuel 66, 170-178.
3. Alfrey, T., Gurnee, E. F. and Lloyd, W. G., 1966: "Diffusion in glassy Polymers"; Journal of Polymer Sciences (C) 12, 249-261.
4. Peterlin, A., 1977: "Plastic deformation of crystalline polymers"; Polymer Engineering and Science 17, 183-193.
5. Thomas, N., Windle, A., 1982: "A theory of case II diffusion"; Polymer 23, 529--542.
6. Vrentas, J.S., Jarzebski, C.M., Duda, J.L., 1975: "A Deborah number for diffusion in polymer--solvent systems"; AIChE J 21, 894--901.

7. Vrentas, J. S., Duda, J. L., 1977: "Diffusion in polymer-solvent systems. III. Construction of Deborah number diagrams"; *J. Polym. Sci. Polym. Phys. Ed.* 15, 441-453.
8. Lasky, R.C., Kramer, E.J., Hui, C-Y., 1988: "The initial stages of Case II diffusion at low penetrant activities"; *Polymer* 29, 673-679.
9. Gall, T.P., Kramer, E.J., 1991: "Diffusion of deuterated toluene in polystyrene"; *Polymer* 32, 265-271.
10. Hui, C.-Y., Wu, K.-C., Lasky, R. C. and Kramer, E. J., 1987: "Case-II diffusion in polymers. I. Transient swelling"; *Journal of Applied Physics* 61, 5129-5136.
11. Hui, C.-Y., Wu, K.-C., Lasky, R. C. and Kramer, E. J. 1987: "Case-II diffusion in polymers. II. Steady-state front motion"; *Journal of Applied Physics* 61, 5137-5149.
12. Govindjee, S., Simo, J.C., 1993: "Coupled stress-diffusion: Case II"; *J. Mech. Phys. Solids* 41, 863-887.
13. Durning, C., 1985: "Differential sorption in viscoelastic-fluids"; *Journal of Polymer Sciences (B)* 23, 1831--1855
14. Argon, A.S., Cohen, R.E., Patel, A.C., 1999: "A mechanistic model of case II diffusion of a diluent into a glassy polymer"; *Polymer* 40, 6991-7012.
15. Crank, C.J., 1976: The mathematics of diffusion: Oxford University Press, Oxford.
16. Jou, D., Casas-Vazquez, J., Lebon, G., 2001 : Extended Irreversible Thermodynamics: Springer-Verlag, Heidelberg.
17. Landau, L.D., Lifshitz, E. M., 1975: Fluid Mechanics: Pergamon Press. Oxford.

Diffusional exponent (n)			De	Transport mechanism
Plane sheet	Cylinder	Sphere		
0.5	0.45	0.43	$\gg 1$ or $\ll 1$	Fickian
$1.0 > n > 0.5$	$0.89 > n > 0.45$	$0.85 > n > 0.43$	0	Anomalous
1.0	0.89	0.85	1.0	Case II
$n > 1.0$	$n > 0.89$	$n > 0.85$	-	Super case II

Table 1. Dependence of diffusion exponent on sample geometry

Sample	Warndt Luisenthal
Carbon [%]	81.3
Hydrogen [%]	5.58
Nitrogen [%]	1.88
Sulphur [%]	0.69
Oxygen (diff.) [%]	5.47
H/C	0.82
O/C	0.05
Rmax [%]	0.71
Vitrinite [%]	74.4
Liptinite [%]	15.6
Inertinite [%]	9
Minerals [%]	1
Specific surface [m^2/g]	104
Micropore volume [cm^3/g]	0.03545
Diameter [mm]	74.48
Length [mm]	154

Table 2. Sample properties

Parameter	
D_g	$10^{-11} \text{ m}^2/\text{s}$
D_r	$10^{-10} \text{ m}^2/\text{s}$
m	10-30
T_g	350°C
Ω	$1.68 \times 10^{-29} \text{ m}^3/\text{molecule}$
η_0	10^{15} Ns/m^2
Φ_0	0.205
Φ_c	$0.10 \times \Phi_0$
Length	10^{-2} m
T	45°C

Table 3. Parameters used in simulation for a CO_2 – coal system.

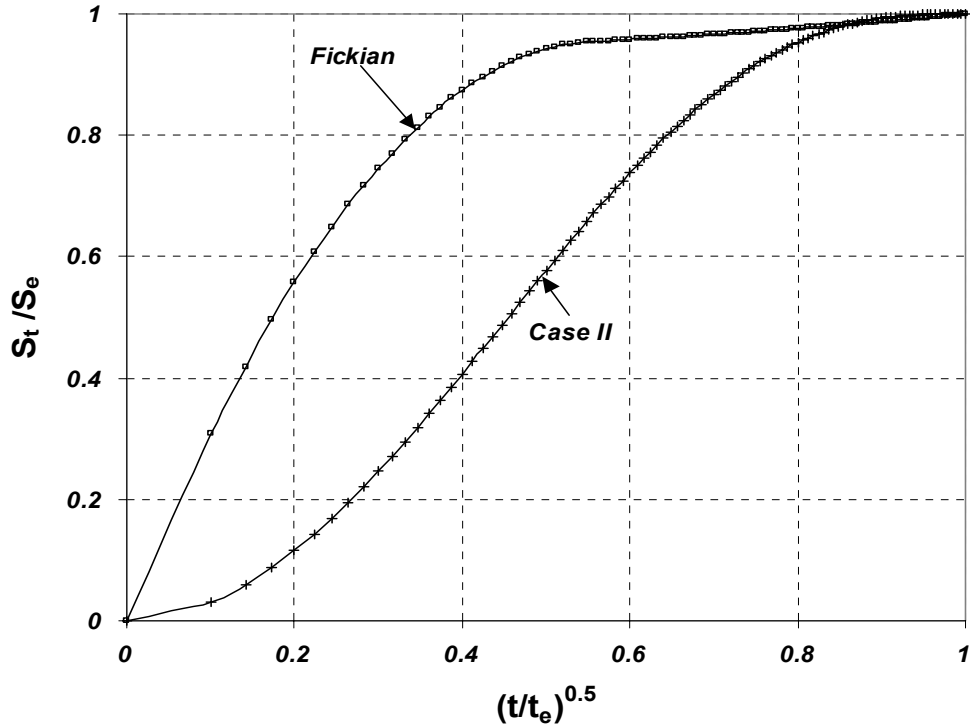


Figure 1 Generalized plots of the dynamic volumetric swelling, plotted as dimensionless mass uptake vs. square root of dimensionless time for limiting Fickian and relaxation controlled Case II diffusion in a spherical particle

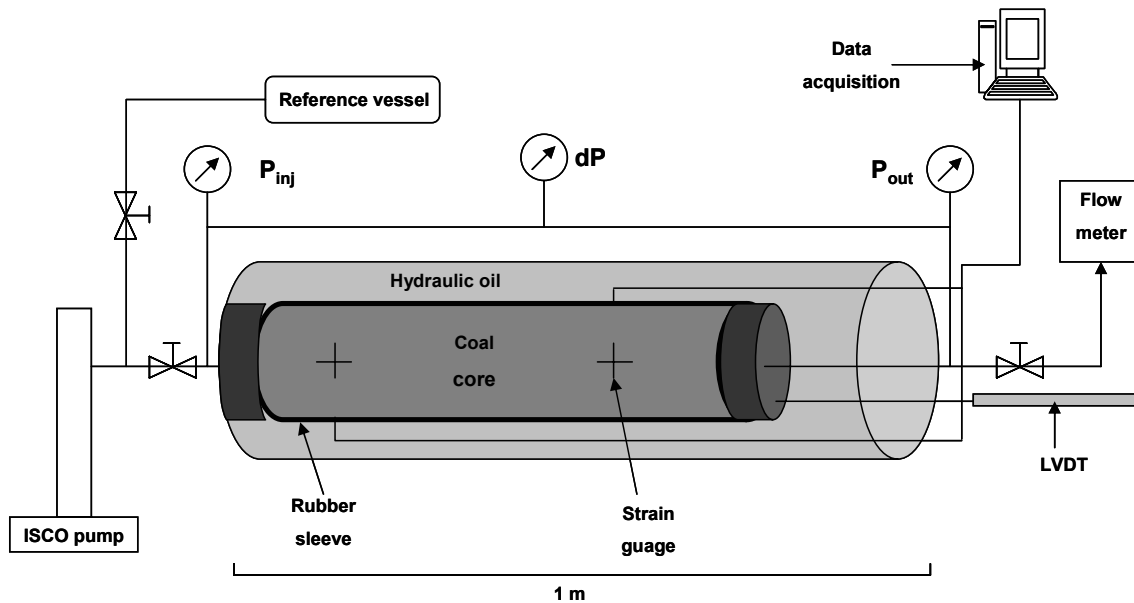


Figure 2 Schematic of the high pressure Dynamic Volumetric Swelling setup

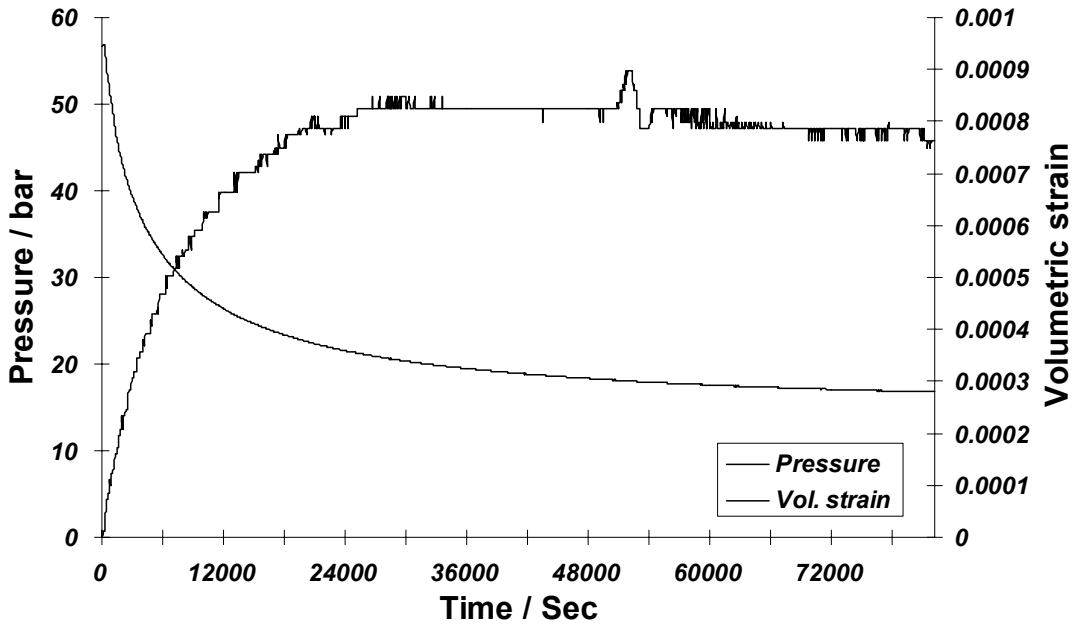


Figure 3 Dynamic Volumetric Swelling (DVS), plotted as the volumetric strain and the pressure against time from the first pressure step of the swelling experiment on Warndt Luisenthal coal (0.71% R_{max}) at 45°C with CO₂

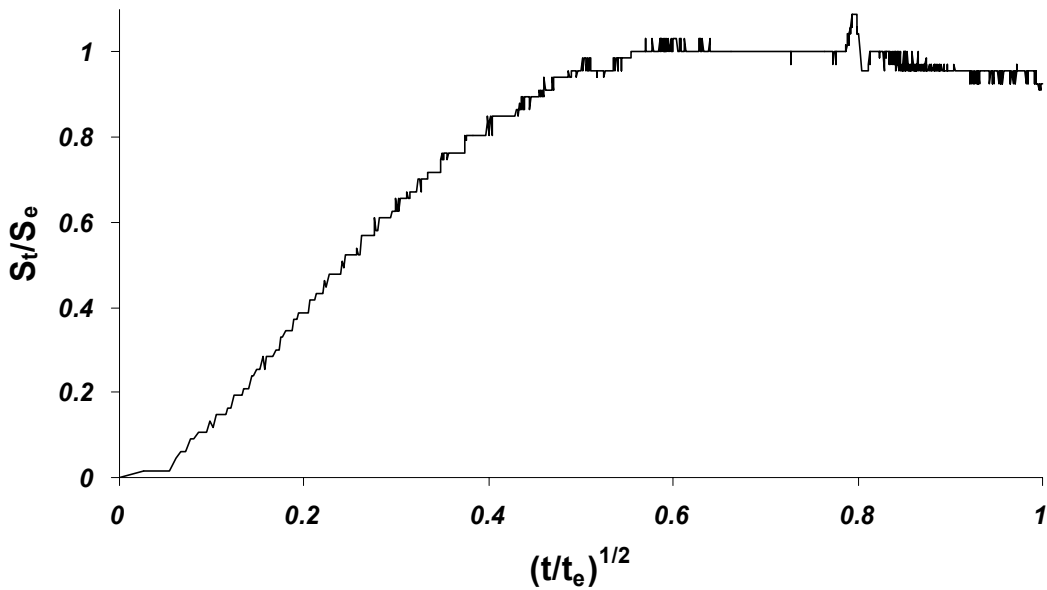


Figure 4 Plot of the Dynamic Volumetric Swelling, plotted as dimensionless mass uptake against the square root of dimensionless time from the swelling experiment of Warndt Luisenthal coal (0.71% R_{max}) at 45°C with CO₂

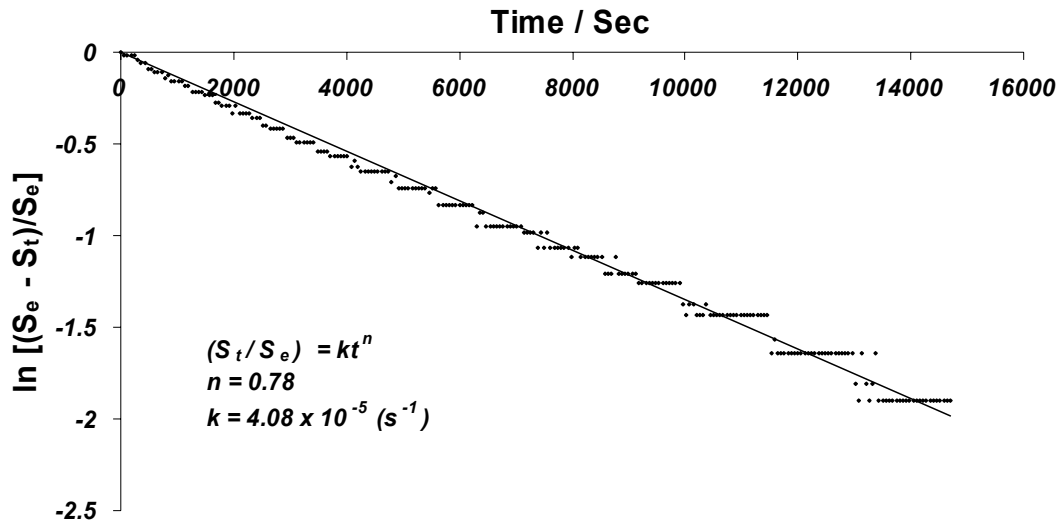


Figure 5 Variations of $\ln[(S_e - S_t)/S_e]$ with time for the swelling of Warndt Luisenthal coal (0.71% R_{\max}) at 45°C with CO₂

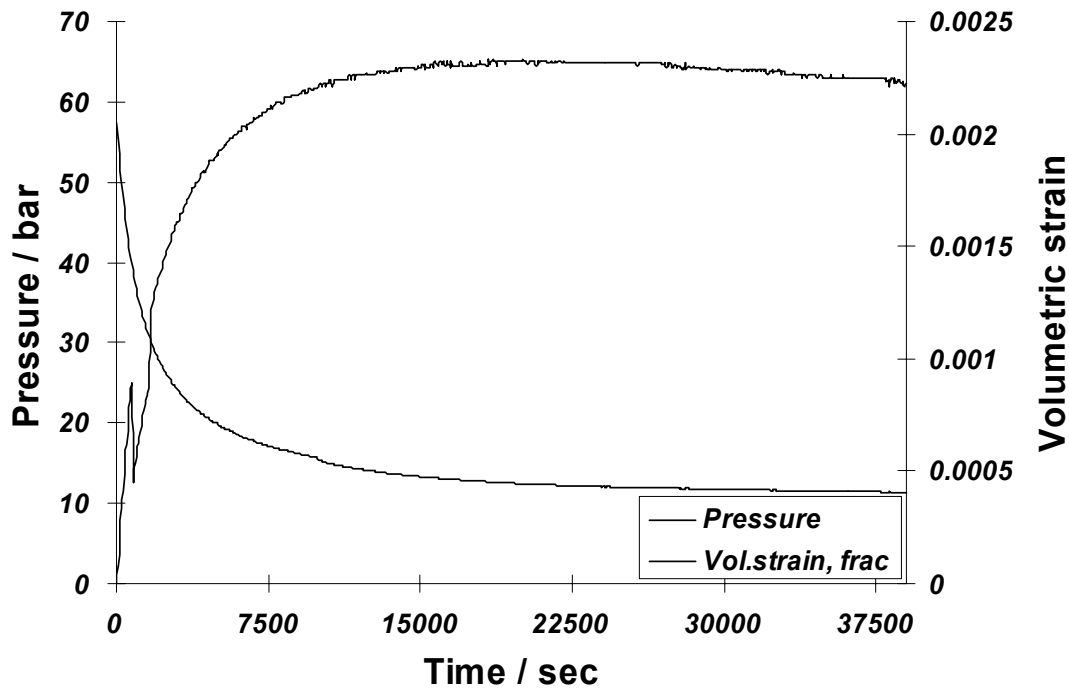


Figure 6 Dynamic Volumetric Swelling (DVS), plotted as the volumetric strain and the pressure against time from the first pressure step of the repeat swelling experiment on Warndt Luisenthal coal (0.71% R_{\max}) at 45°C with CO₂

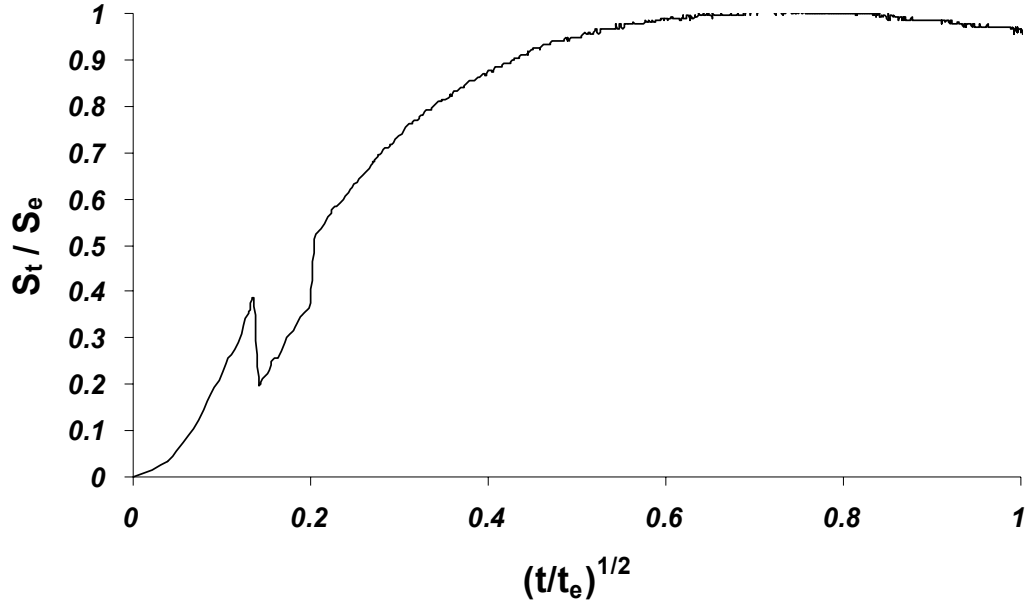


Figure 7 Plot of the Dynamic Volumetric Swelling, plotted as dimensionless mass uptake against the square root of dimensionless time from the repeat swelling experiment of Warndt Luisenthal coal (0.71% R_{max}) at 45°C with CO_2

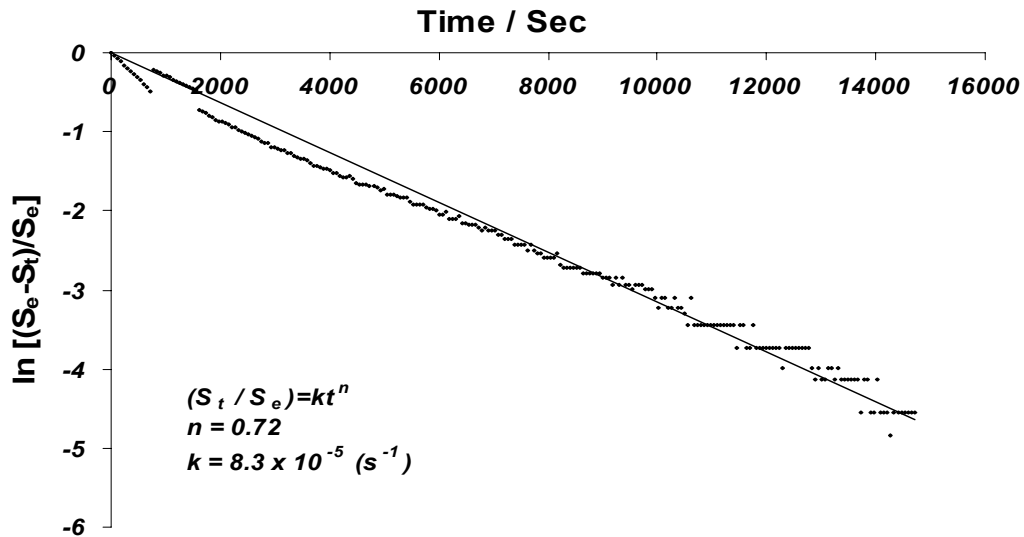


Figure 8 Variations of $\ln[(S_e - S_t)/S_e]$ with time for the repeat swelling of Warndt Luisenthal coal (0.71% R_{max}) at 45°C with CO_2

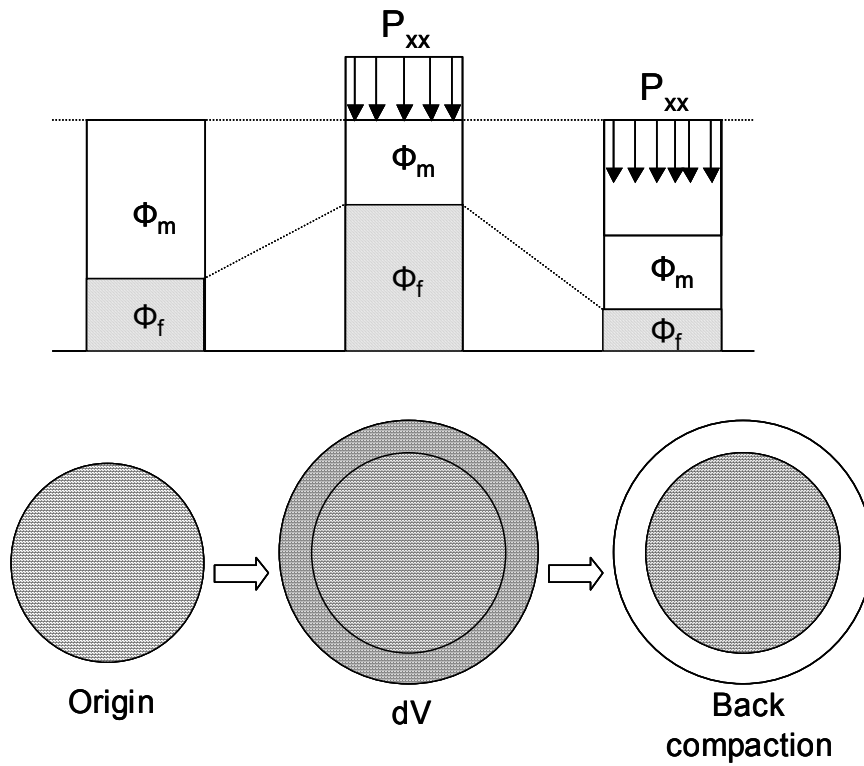


Figure 9 Concept of swelling stress

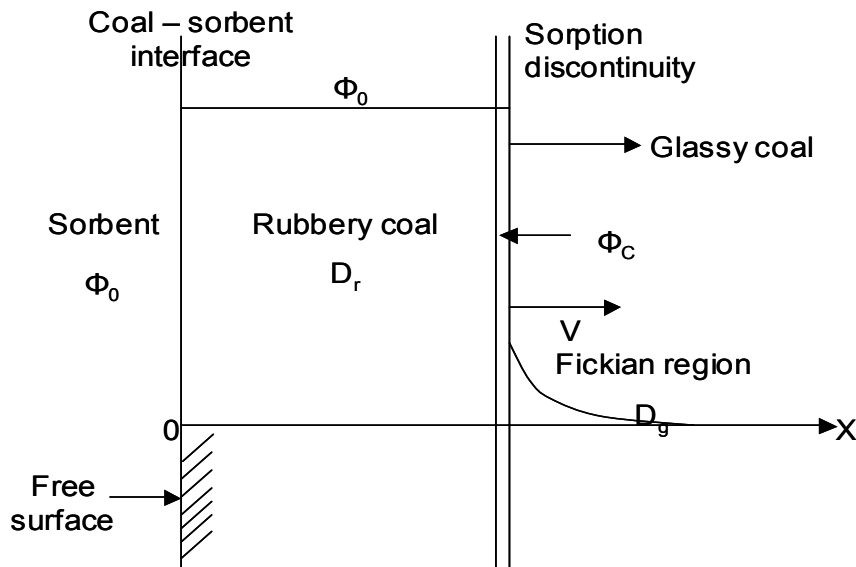


Figure 10 Idealized concentration profile proposed by Argon et al. (1999) for Case II sorption into an infinite sheet with a Fickian diffusion front preceding the advancing boundary between swollen rubbery and the essentially unpenetrated glassy coal

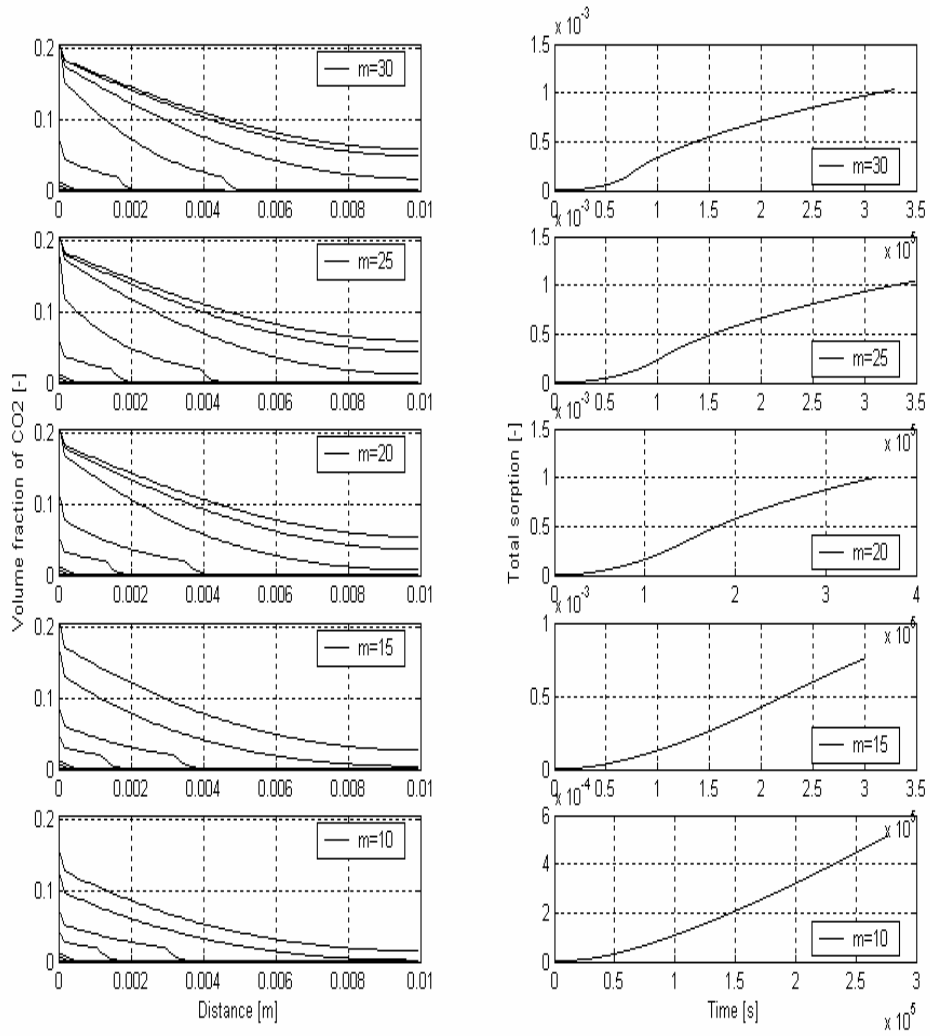


Figure 11 Effect of varying m (10 to 30) on the calculated Case II profiles and total sorption. The parameters used to run the simulations are shown in Table. 3.